scientific reports

OPEN

Evaluation method of interface bonding strength of cemented carbide with additives

Chen Wang[1,2], Ziqiang Pi[1,2], Zhaoran Zheng[1,2], Xing Chen[1,2] & Kaiping Du[1,2]✉

Cemented carbides are widely used in cutting tools, wear-resistant parts and other fields. In order to further improve the mechanical properties, additives are usually added to cemented carbides. The interface bonding strength of additives with WC and Co phases will affect the crack propagation and have an important influence on the mechanical properties of cemented carbides. The gradient of electron work function (EWF) at the interface of WC/additive and Co/additive were obtained by atomic force microscope in this paper. According to the numerical relationship between the gradient of EWF and the interface bonding strength, the interface bonding strength of different additives and cemented carbide were qualitatively studied. The results show that in the interface of WC/additives, the interface bonding strength of WC/VC is the largest, followed by WC/TiC and WC/ZrO_2. In the interface of Co/additives, the interface bonding strength of Co/VC is the largest too, followed by Co/ZrO_2 and Co/TiC, which verified the feasibility of this method in the field of cemented carbide.

Keywords Cemented carbide, Additives, Interface bonding strength, Electron work function

Cemented carbide is a kind of composite material made by powder metallurgy process, which is mainly composed of refractory metal carbides and bonded metals[1,2]. This material has high strength, hardness and wear resistance, but also has a certain toughness, playing an indispensable role in promoting industrial manufacturing and economic development[3–5]. Among the cemented carbides with different compositions, WC-Co cemented carbide has the best comprehensive performance, so it is widely used in the manufacture of various tools and equipment, including cutting, mining and drilling tools, as well as wear-resistant parts and extrusion molds. Dewangan et al. analyzed the critical damage state of WC-Co cone tip during service, and found that the failure of the cone tip was mainly due to the cracking and crushing of WC grains[6]. By analyzing the critical wear state of WC-Co-Based Twist Drill Bits in service, it is found that the failure of Twist Drill Bits is due to the crack in WC grains, which leads to grain breakage and the formation of voids[7]. With the continuous improvement of material performance requirements in the industrial manufacturing field, in order to improve the service life of tools, higher requirements are also put forward for the comprehensive mechanical properties of cemented carbides.

Studies have shown that adding a small number of additives to cemented carbide, such as VC, Cr_3C_2, NbC, TiC, TaC, etc.[8–14] can significantly improve its mechanical properties, especially hardness. In recent years, ZrO_2 is also often used as an additive to improve the toughness of cemented carbide[15,16]. These additives are easy to aggregate at the WC/WC and WC/Co interfaces. For example, VC is easy to enrich at the WC/Co interface, and VC segregation occurs, which makes the grain size of the cemented carbide significantly reduced[17]. ZrC does not segregate and separates into phases at the triple junction, which improves the hardness of the cemented carbide[17,18]. TiC will inhibit grain growth and reduce grain size. At the same time, TiC will form (W, Ti) C solid solution with WC, forming a core-shell structure with TiC inside and (W, Ti) C outside, which will improve the hardness of cemented carbide, but the toughness is low[19]. Adding an appropriate amount of NbC can reduce the grain size. WC dissolves into NbC to form (Nb, W) C solid solution, which can improve the hardness of cemented carbide, but the fracture toughness and bending strength are reduced[20]. After adding additives, whether it is to form a new phase or reduce the grain size, the number of interfaces and interface properties in cemented carbides are changed, and the failure of cemented carbides, especially ultrafine-grained cemented carbides, is mainly intergranular fracture[21]. Therefore, the strength of the interface bonding strength greatly affects the mechanical properties of the material.

At present, the test method of macroscopic interface bonding strength[22–24] is mainly to evaluate the interface bonding quality of the alloy by observing the microstructure after interface failure or by bending and stretching. However, the content of additives in cemented carbides is small, and the size of additives formed or precipitated

[1]BGRIMM TECHNOLOGY GROUP, Beijing 100160, China. [2]BGRIMM Advanced Materials Science & Technology Co., Ltd, Beijing 102206, China. ✉email: dukaiping@bgrimm.com

phases is only micron or nanometer. Therefore, the traditional method cannot determine the micro-interface bonding strength formed by the additives with WC and Co phases. The bonding strength of the micro-interface can be evaluated by first-principles calculation and finite element simulation technology[25–27]. For example, Yin et al.[25] established the healing degree model of the interface by finite element method, studied the influence of different process parameters on the interface bonding strength, and input the data into the machine learning model. The quantitative analysis results of process parameters on interface bonding strength were obtained by combining finite element method and machine learning method. Li et al.[26] calculated the atomic bond strength of different interfaces by first-principles calculation method, and found that the atomic bond strength of W-Fe interfaces is the largest, then W-Co and W-Ni, and studied the interface bonding strength of different cemented carbide interfaces. However, this simulation calculation method is difficult to analyze and model, and it is usually carried out under ideal conditions, with certain errors.

Since the interface bonding of metal materials is related to the electronic behavior at the interface[28], most of the interface bonding strength can be judged according to the electron work function (EWF), but there are special cases[29]. The interface EWF gradient method[30] is a new evaluation method that can qualitatively study the interface bonding strength. The EWF is an electron with an initial energy equal to the Fermi level, and the minimum energy required to escape from the inside of the metal to the vacuum.

$$\phi = -(eV_e + \epsilon_e^F)$$

Here, ϕ is EWF, V_e is the electric potential, and ϵ_e^F is the Fermi kinetic energy.

According to the above formula, the EWF difference ($d\phi$) can be obtained by testing the phase surface potential difference (dV_e). Studies have shown that the gradient value of the EWF at the interface has a great correlation with the interface bonding strength: the smaller the gradient value, the higher the interface bonding strength, the larger the gradient value, and the lower the interface bonding strength[30,31].

This paper evaluated the interface bonding strength between the additive forming phase and WC or Co phases by calculating the interface EWF gradient, and the feasibility of this method in the field of cemented carbide is determined by comparing with the previous research results.

Materials and methods

In this paper, nano-WC-Co composite powder and Co powder were mixed with different additives (commonly used carbide VC, TiC, and ZrO_2 that can toughen cemented carbide by phase transition) according to the stoichiometric ratio of ball milling with anhydrous ethanol as the ball milling medium. Among them, C powder, Co_3O_4 powder and $WO_{2.9}$ powder are the raw materials for the preparation of nano-WC-Co composite powder. The scanning electron microscope images of the raw materials in this study are shown in Fig. 1a-e. The mixed powder was dried, sieved, mixed with glue, cold pressed and sintered (Ar atmosphere at 6 MPa for 60 min.) to prepare cemented carbide with different additives, the sample obtained is shown in Fig. 1f.

The sample is cut and then grinded and polished to make the surface of the sample smooth. The phase analysis of the samples was carried out by X-ray diffractometer, the microstructure of the samples and the content and

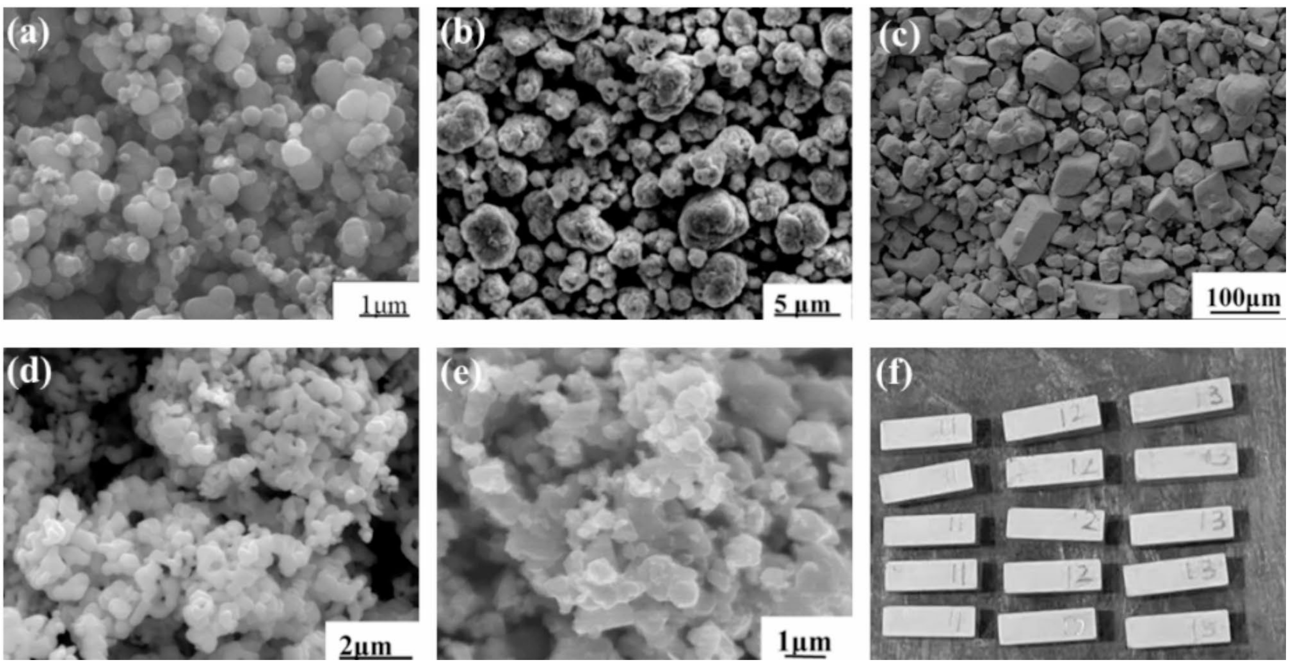

Fig. 1. (**a-e**) SEM of C powder, Co_3O_4 powder, $WO_{2.9}$ powder, Co powder, TiC powder and (**f**) images of cemented carbide samples.

distribution of various elements were observed by scanning electron microscope and energy spectrum, and the surface potential and magnetic phase angle of each phase in the sample were tested by atomic force microscope.

Result and discussion

Microstructure and interface bonding strength of cemented carbide with ZrO_2 additive

According to the difference of physical properties between the additives phase, Co phase and WC phase, the difference in SEM morphology and surface potential, the test results were analyzed.

Figure 2a is the XRD pattern of cemented carbide with ZrO_2 as additive. The calibration of the diffraction peaks shows that the prepared cemented carbide is composed of WC[32], Co[33] and ZrO_2[34] phases. Figure 2b shows the SEM image of the cemented carbide containing ZrO_2. The microstructure is relatively uniform and the WC grains are round. The EDS results shown in Fig. 3 confirm again that there are WC, Co and ZrO_2 phases in the sample. In Fig. 2b, the bright area is WC, the black area is Co phase, and the gray area is ZrO_2, which is formed in a slender strip and easily appears around the Co phase. It can be seen that WC-Co cemented carbide with ZrO_2 phase were prepared by using the process route designed in this paper, which laid a foundation for the determination of the bonding strength between additives and WC and Co interfaces.

Figure 4a-c shows the morphology, magnetic phase angle distribution and surface potential distribution of cemented carbide obtained under atomic force microscope. The color of the morphology is related to the surface height of the specimen. The white bright color area is a high-altitude area, and the black area is a low-lying area. Because the Mohs hardness of WC, Co and ZrO_2 are 9,5.5 and 8.5, respectively, the Co phase is easy to be polished to become the lowest region, followed by the ZrO_2 phase. Therefore, the white area in Fig. 4a is WC, the black area is Co, and the brown area is ZrO_2. The Co phase is a ferromagnetic material. Therefore, the magnetic phase angle distribution of the alloy was measured by AFM magnetic force microscope (as shown in Fig. 4b), where the dark area is the Co phase. The surface potential distribution diagram can reflect the relative potential of the cemented carbide, that is: surface potential = probe tip potential-phase potential. Therefore, the higher the phase potential, the darker the brightness displayed in the diagram. Because the Co phase has a lower potential (− 0.93 V), and the WC phase has a higher potential (− 0.53 V), the contrast of the WC phase in the surface potential diagram is darker, and the Co phase is brighter ; the location of WC, Co and ZrO_2 phases can be determined by comprehensive analysis (as shown in Fig. 4).

Figure 4d shows the EWF curve at the position shown by the solid line. According to Fig. 4d, the EWF of WC, Co and ZrO_2 can be obtained. The EWF gradient at the interface (such as WC/ZrO_2, Co/ZrO_2 and WC/Co) can be expressed by the slope of the EWF at the interface. In order to obtain accurate data, at least 6 sets of data are calculated for the EWF gradient of each interface. The results obtained by averaging are shown in Table 1. It can be seen that compared with the EWF gradient of the WC/Co interface of 66.92 ± 4.32 mV/μm, the WC/ZrO_2 interface is 264.93 ± 6.77 mV/μm, which is much higher than the WC/Co interface EWF gradient, while the Co/ZrO_2 interface is 108.01 ± 4.53 mV/μm, which is higher than the WC/Co interface EWF gradient. That is to say, in this sample, the interface bonding strength of WC/ZrO_2 is the lowest, and the interface bonding strength of WC/Co is the highest, that is, the interface bonding strength from high to low is: WC/Co, Co/ZrO_2, WC/ZrO_2.

Microstructure and interface bonding strength of cemented carbide with VC additive

Figure 5 shows the XRD and SEM images of cemented carbide with VC as additive. It can be seen that the prepared cemented carbide is composed of WC, Co and VC[35] phases, and the WC grain size is not uniform.

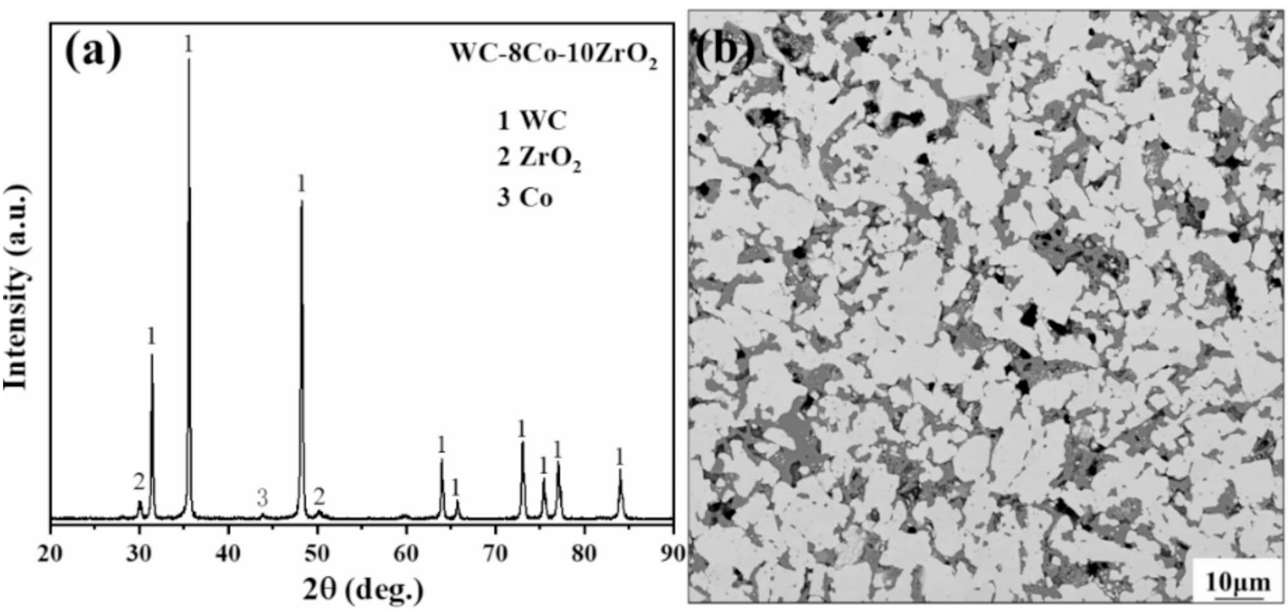

Fig. 2. (**a**) XRD and (**b**) SEM of cemented carbide with ZrO_2 additive.

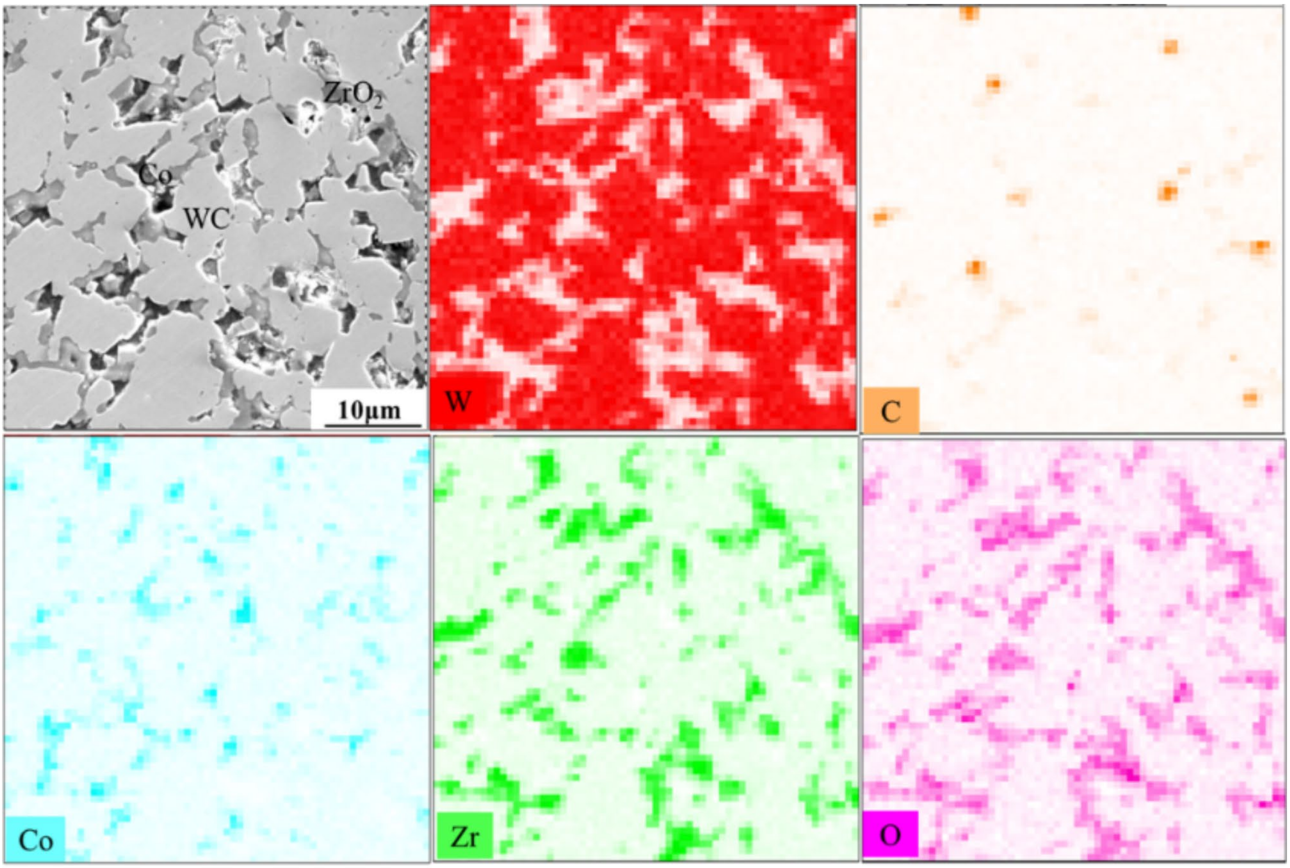

Fig. 3. EDS of cemented carbide with ZrO_2 additive.

Through the EDS analysis shown in Fig. 6, it can be seen that the bright area in Fig. 5 is WC phase, the dark gray area is Co phase, and the light gray area is VC phase. Combining the two characterization results, it can be observed that VC aggregates to form a large VC phase, while Co phase is dispersed in the gap between grains.

Figure 7a-c is the morphology, magnetic phase angle distribution and surface potential distribution of cemented carbide obtained by AFM. The distribution of each phase can be obtained by using the same analysis method as the cemented carbide with ZrO_2 as the additive. The darker phase in Fig. 7b and the brighter phase in Fig. 7c are Co phase, and the darkest phase in Fig. 7c is VC phase, as shown in Fig. 6.

Figure 7d is the EWF at the corresponding position of the straight line in Fig. 7a-c. The EWF gradients of WC, Co and VC interfaces (such as WC/VC, Co/VC and WC/Co) can be obtained as shown in Table 2. It can be seen that the EWF gradient of the WC/Co interface is 40.94 ± 1.25 mV/μm, the WC/VC interface is 22.40 ± 2.81 mV/μm, and the Co/VC interface is 51.59 ± 1.36 mV/μm. The slope of the EWF of the Co/VC interface is the largest, indicating that the interface bonding strength of the Co/VC is the lowest, and the interface bonding strength of the WC/VC is the highest. That is: the interface bonding strength from high to low interface is: WC/VC, WC/Co, Co/VC.

Microstructure and interface bonding strength of cemented carbide with tic additive

Figure 8 is the XRD and SEM images of cemented carbide with TiC as additive. It can be seen from Fig. 8a that the prepared cemented carbide is composed of WC, Co and TiC[36] phases, while the scanning electron microscope diagram of Fig. 8b shows that the microstructure of the sample is relatively uniform, and the WC grains have no fixed form, but there are four phases. It can be seen from the EDS analysis shown in Fig. 9 that there are four phases of WC, Co, TiC and (Ti, W) C in the sample. Most of the TiC phase is surrounded by the (Ti, W) C phase, and only a very small part is in contact with the WC phase. The Co phase easily appears at the interface between WC and (Ti, W) C.

Figure 10a-c is the morphology, magnetic phase angle distribution and surface potential distribution of cemented carbide obtained under AFM. The analysis shows that Co phase is the darker phase in Fig. 10b coincides with the brighter phase in Fig. 10c. According to EDS analysis, most of the TiC phase is surrounded by (Ti, W) C phase, so the darkest phase in Fig. 10c is more likely to be (Ti, W) C, as shown in Fig. 10.

Figure 10d is the EWF at the position corresponding to the straight line position of Fig. 10a-c, from which the EWF gradient of WC, Co and (Ti, W) C interfaces (such as WC/ (Ti, W) C, Co/ (Ti, W) C and WC/Co) can be obtained as shown in Table 3. It can be seen that the EWF gradient of the WC/Co interface is 66.46 ± 2.52 mV/μm, the WC/ (Ti, W) C interface is 73.49 ± 4.84 mV/μm, and the Co/ (Ti, W) C interface is 115.06 ± 10.81 mV/

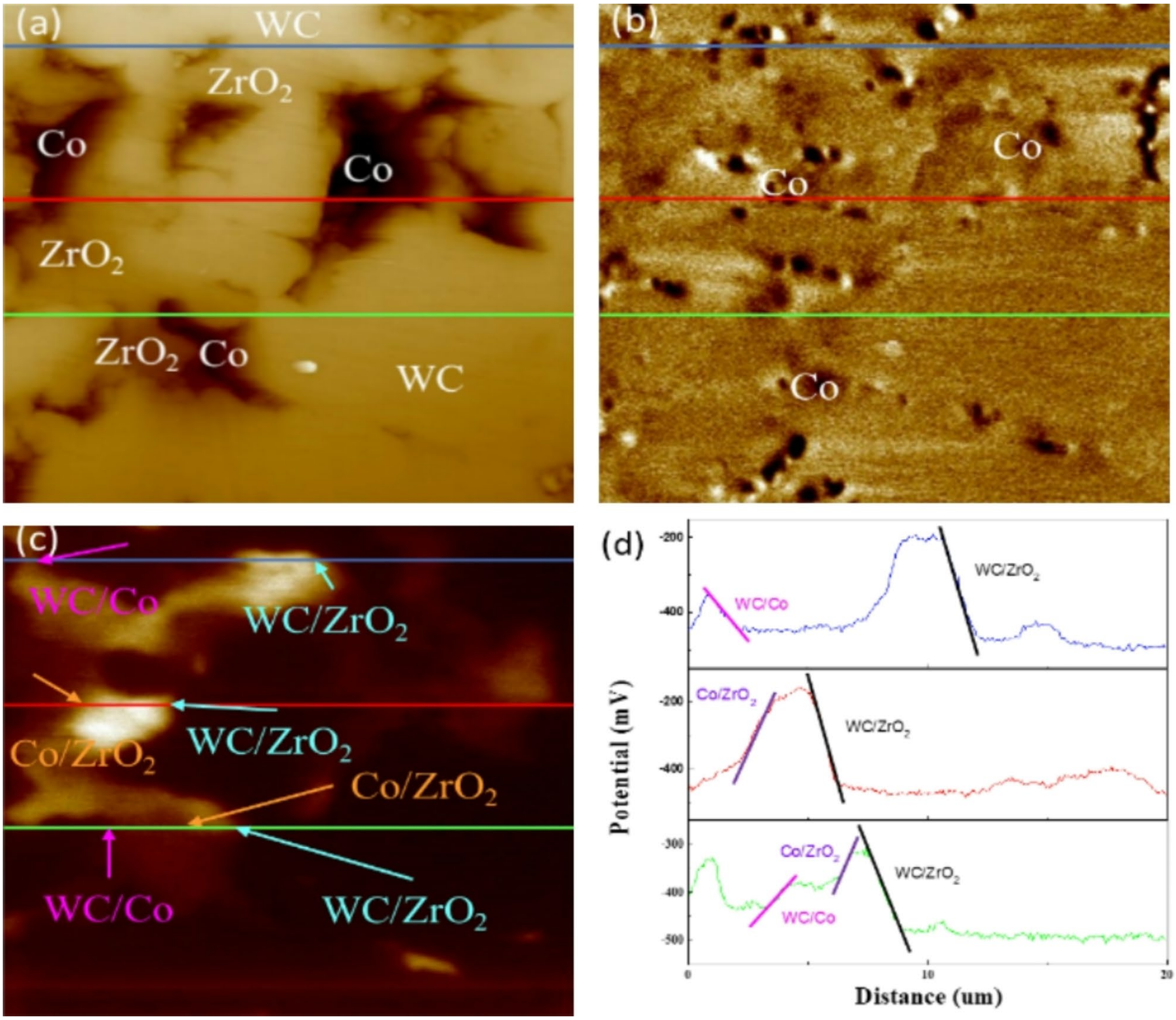

Fig. 4. AFM images of cemented carbide with ZrO_2 additive: (**a**) morphology, (**b**) magnetic phase angle, (**c**) surface potential diagram, (**d**) the EWF curve at the position shown by the solid line.

Interfaces	WC/Co	WC/ZrO_2	Co/ZrO_2
EWF gradient (mV/μm)	66.92 ± 4.32	264.93 ± 6.77	108.01 ± 4.53

Table 1. EWF gradient at different interfaces of cemented carbide with ZrO_2 additive.

μm. The EWF slope of the Co/ (Ti, W) C interface is the largest, indicating that the interface bonding strength of the Co/ (Ti, W) C is the lowest, and the interface bonding strength of the WC/Co is the highest. That is : the interface bonding strength from high to low interface is: WC/Co, WC/ (Ti, W) C, Co/ (Ti, W) C.

Comparison of interface bonding strength of cemented carbide with different additives

Due to the high hardness of the cemented carbide, the probe will be worn during use, which may cause the change of the tip potential of the probe. In order to ensure the comparability of the data, the gradient of the interface EWF of the WC/Co is used as a benchmark for normalization, and the relative data of the gradient of the interface EWF formed by different additives with Co and WC in the cemented carbide are obtained, as shown in Tables 4 and 5. The analysis shows that the influence of different additives on the interface bonding strength of cemented carbides are different. The interface bonding strength of VC/WC is higher than WC/Co. The interface bonding strength of TiC/WC and ZrO_2/WC is lower than that of WC/Co. The interface bonding strength between Co and additives is lower than that of WC/Co. Johansson et al.[37] used the calculation method

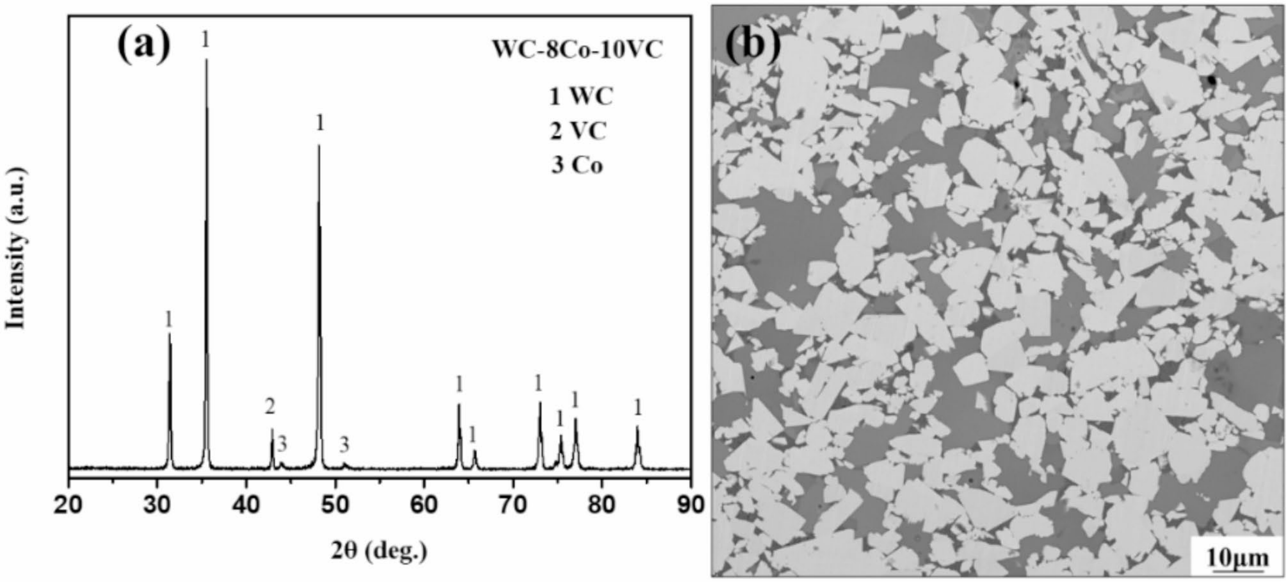

Fig. 5. (**a**) XRD and (**b**) SEM of cemented carbide with VC additive.

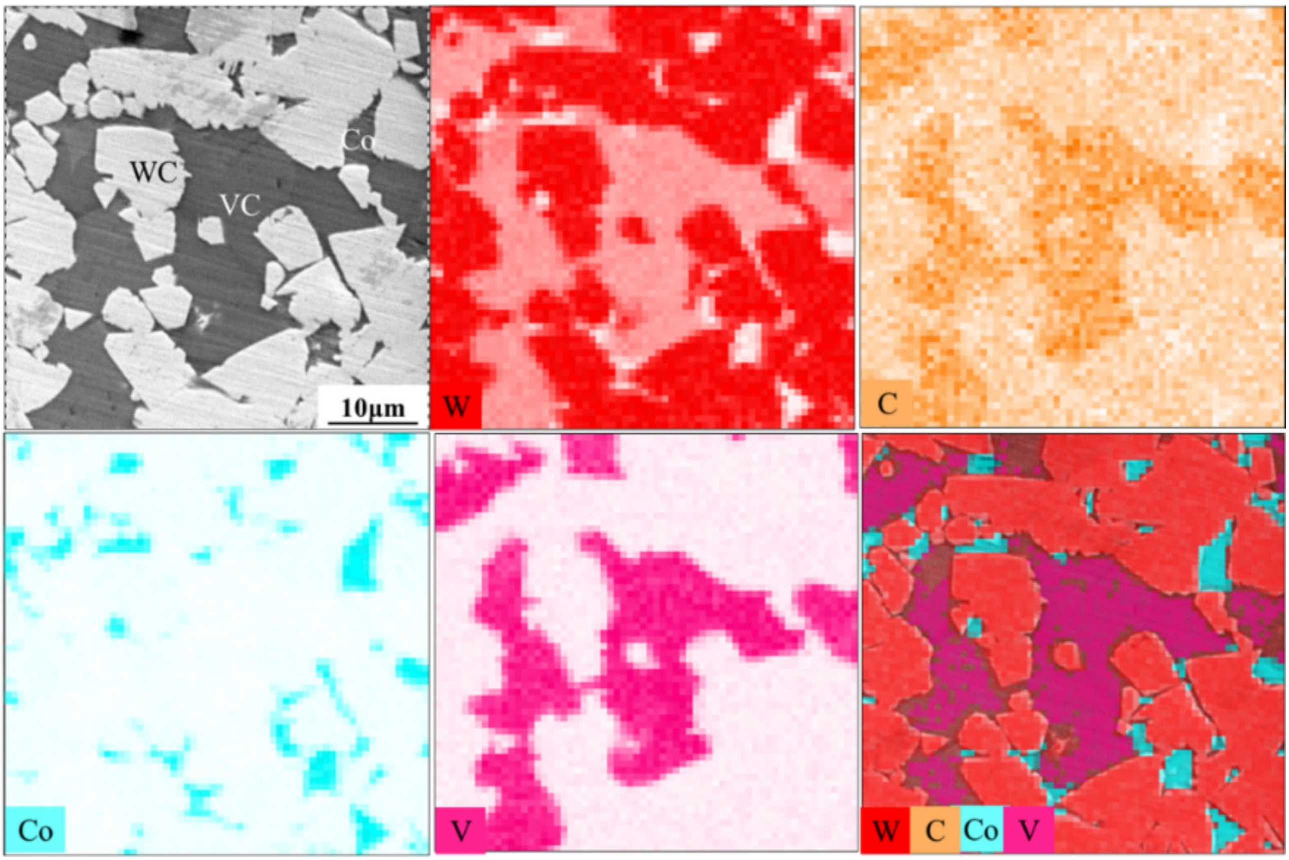

Fig. 6. EDS of cemented carbide with VC additive.

to obtain the result that the interface bonding strength of VC with WC and Co is greater than that of TiC with WC and Co, which is consistent with the measurement results of this project.

It can be seen from the above results that the interface bonding strength between VC and WC is higher, while the interface bonding strength between VC and Co is lower. In the preparation of materials, if VC phase can be more distributed around WC grains and the contact between VC phase and Co can be reduced, materials with

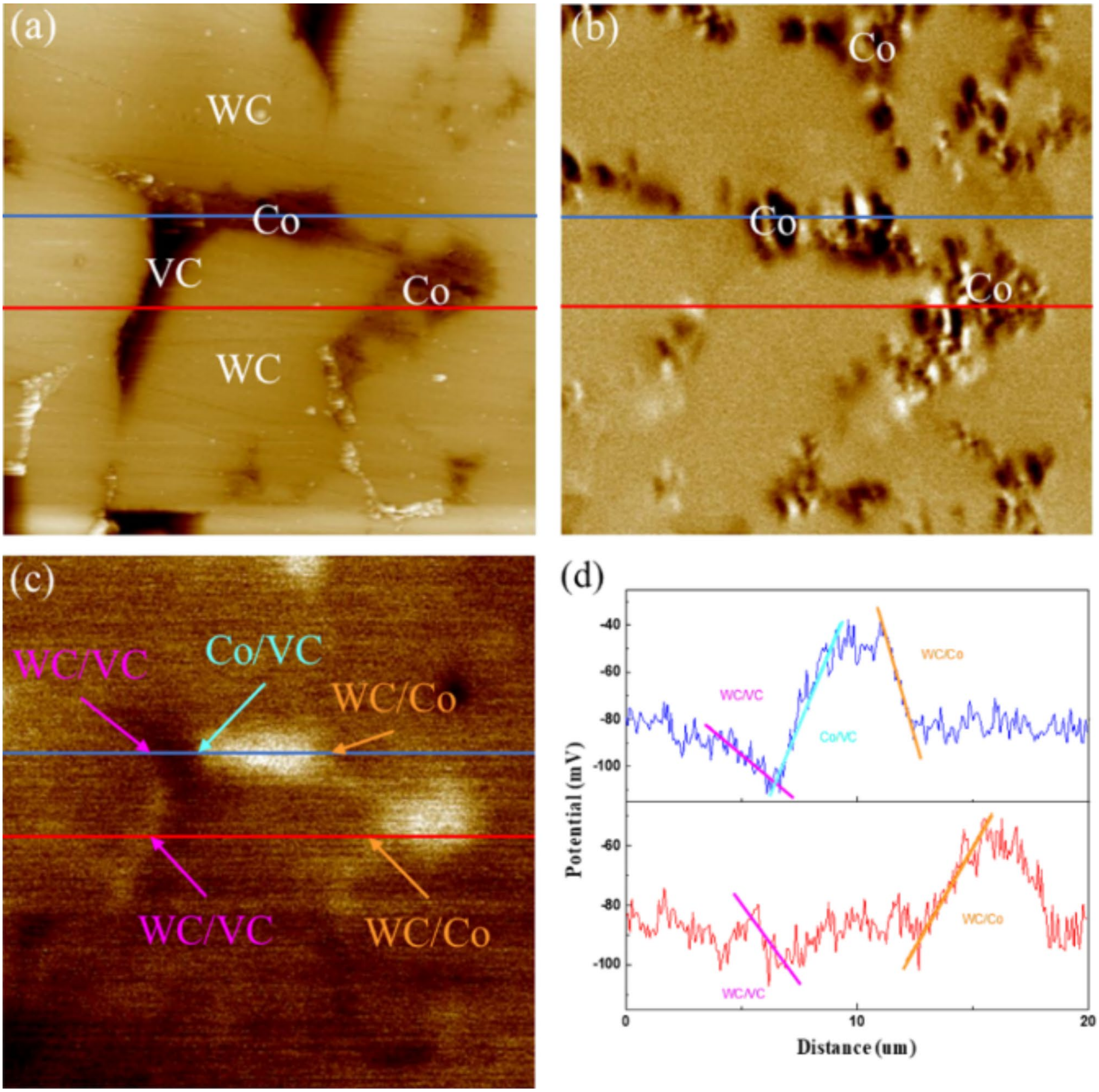

Fig. 7. AFM images of cemented carbide with VC additive: (**a**) morphology, (**b**) magnetic phase angle, (**c**) surface potential diagram, (**d**) the EWF curve at the position shown by the solid line.

Interfaces	WC/Co	WC/VC	Co/VC
EWF gradient (mV/μm)	40.94 ± 1.25	22.40 ± 2.81	51.59 ± 1.36

Table 2. EWF gradient at different interfaces of cemented carbide with VC additive.

better properties may be obtained. Studies have shown that VC is more likely to exist at the interface of WC/WC, and the matching between VC and WC is better[38,39], which is consistent with the results of low gradient of EWF and high interface bonding strength at the interface of VC / WC in this study. Adding VC to cemented carbide can improve its hardness and fracture toughness[40]. Because the interface EWF gradient of TiC/WC is slightly higher and the interface bonding strength is lower, but the addition of TiC in the cemented carbide can reduce the grain size and improve its performance, so the fracture toughness is not significantly reduced[41].

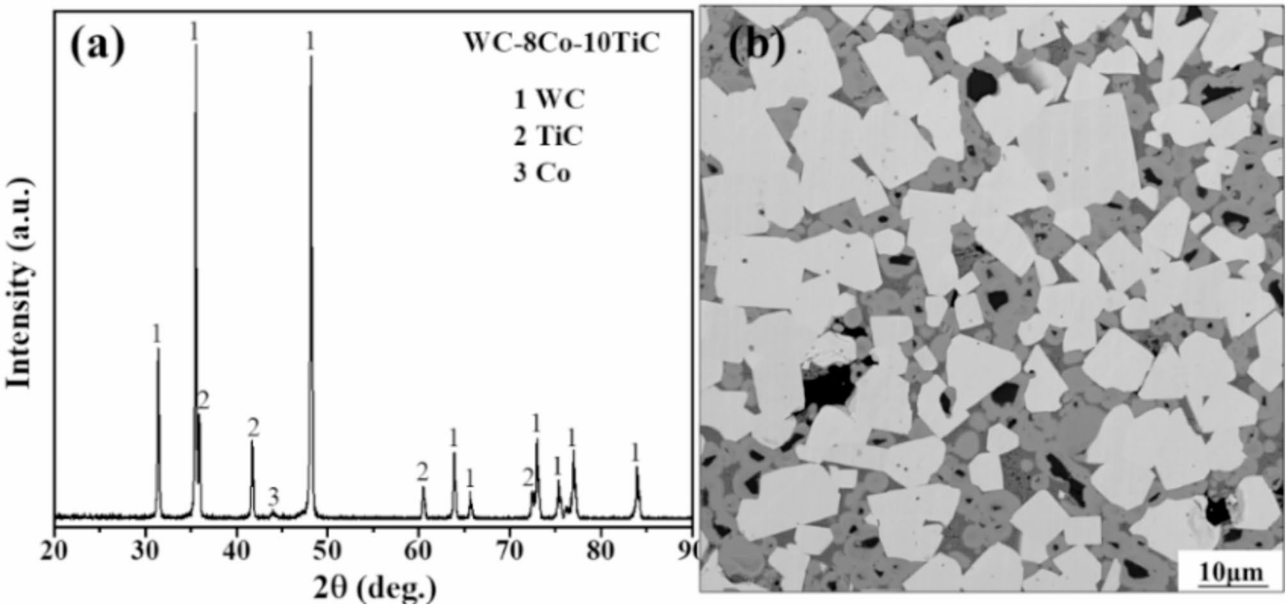

Fig. 8. (**a**) XRD and (**b**) SEM of cemented carbide with TiC additive.

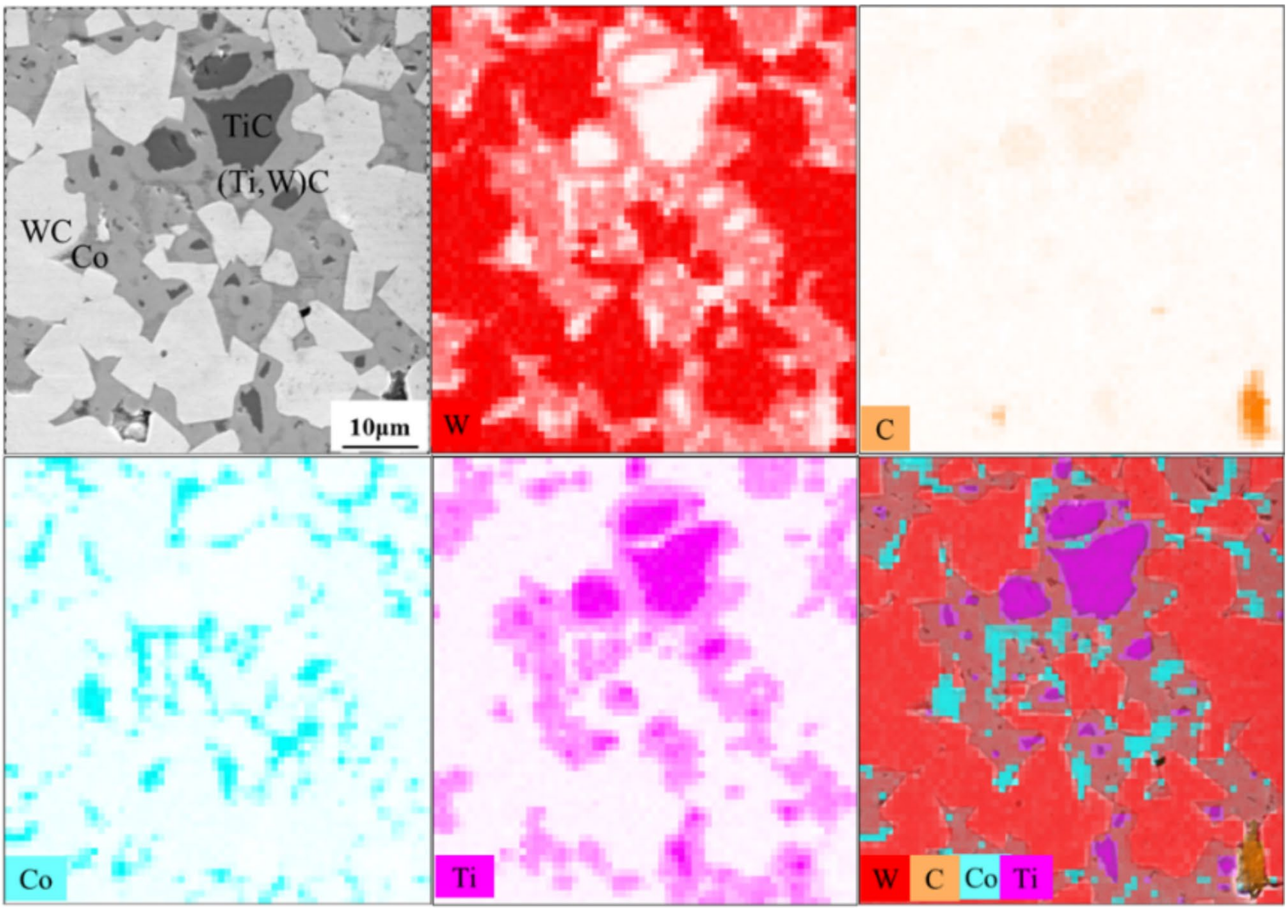

Fig. 9. EDS of cemented carbide with TiC additive.

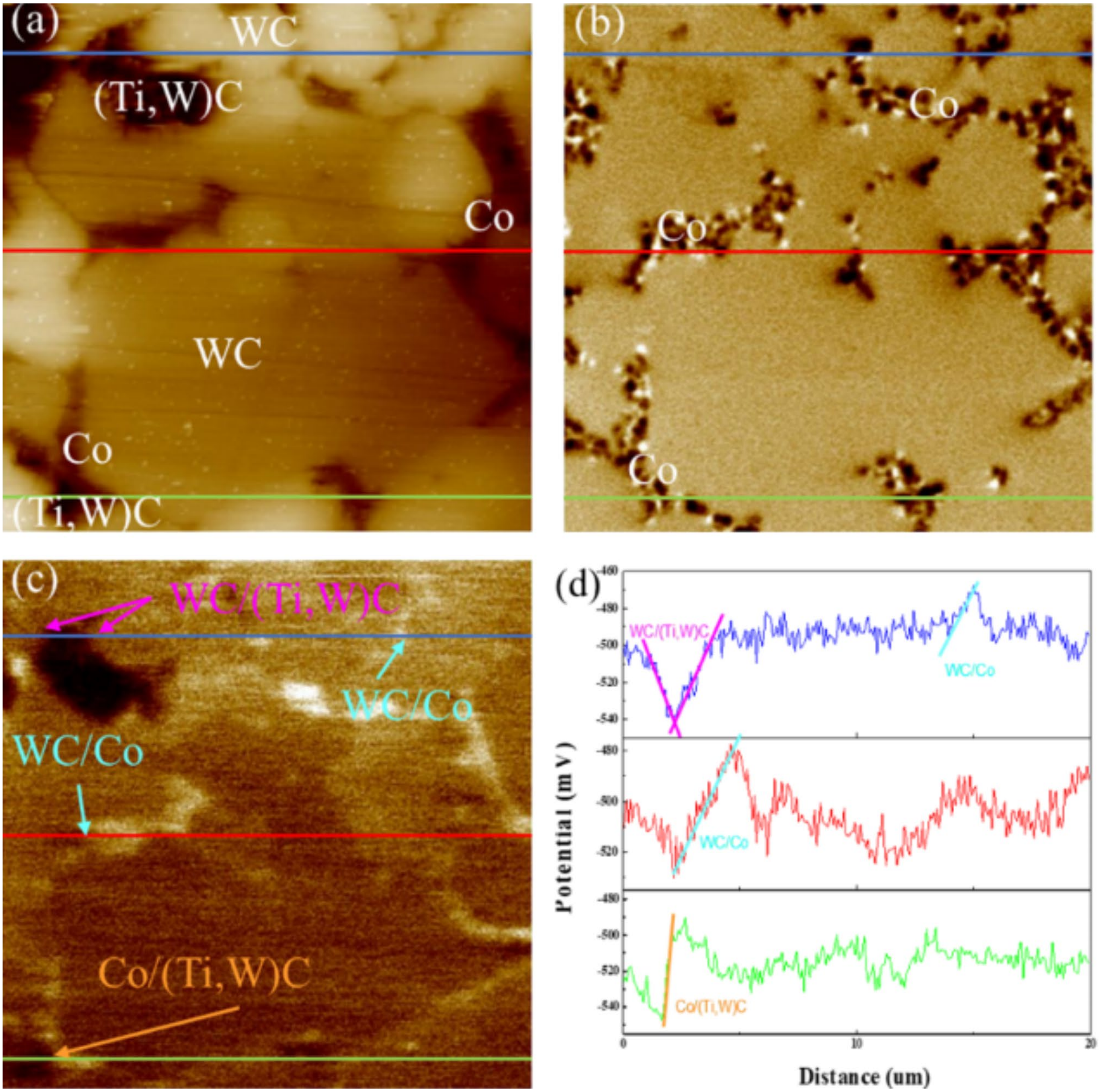

Fig. 10. AFM images of cemented carbide with TiC additive: (**a**) morphology, (**b**) magnetic phase angle, (**c**) surface potential diagram, (**d**) the EWF curve at the position shown by the solid line.

Interfaces	WC/Co	WC/ (Ti, W) C	Co/ (Ti, W) C
EWF gradient (mV/μm)	66.46 ± 2.52	73.49 ± 4.84	115.06 ± 10.81

Table 3. EWF gradient at different interfaces of cemented carbide with tic additive.

Interfaces	WC/Co	WC/TiC	WC/ZrO_2	WC/VC
Normalization results	1	1.11	3.96	0.55

Table 4. Normalization results of interface EWF gradient formed by WC and additives.

Interfaces	WC/Co	Co/TiC	Co/ZrO_2	Co/VC
Normalization results	1	1.73	1.61	1.26

Table 5. Normalization results of interface EWF gradient formed by Co and additives.

This study provides a new method for the evaluation of the interface bonding strength of cemented carbide, and the research results will provide a reference for the selection of additives and the design of high-performance cemented carbide.

Conclusion

Through the preparation of cemented carbide containing different additives, the microstructure of cemented carbide and the distribution of additive phase were observed by XRD, SEM and EDS. The EWF of cemented carbide was measured by atomic force microscope, and the gradient of EWF at the interface was calculated. By comparing the interface between additives and WC and Co phases and the bonding strength of WC/Co interface, the following conclusions were obtained.

(1) The order of interfacial bonding strength is: WC/VC> WC/Co> WC/TiC> WC/ZrO_2, WC/Co> Co/VC> Co/ZrO_2> Co/TiC。
(2) The effect of different additives on the interface bonding strength of cemented carbide was obtained: the interface bonding strength between VC additive phase and WC phase is higher, while the interface bonding strength between TiC, ZrO_2 additive phase and WC phase is lower; the interfacial bonding strength between VC, TiC, ZrO_2 additive phase and Co phase is low.
(3) The research results provide a method to evaluate the interface bonding strength by using the gradient of interfacial EWF, and it can provide guidance for the design of high-performance materials, extending the service life of the workpiece, and has been more widely used in the mining tools, wear parts and other fields.

Data availability

All relevant data are within the paper.

Received: 19 December 2024; Accepted: 25 February 2025
Published online: 04 March 2025

References

1. Tang, X. et al. Preparation, properties and microstructure of high hardness WC-Co cemented carbide tool materials for ultra-precision machining. *Int. J. Refract. Met. Hard Mater.* **116**, 106356 (2023).
2. Wang, Q., Qin, M., Wu, H., Jia, B. & Qu, X. Research status and development trend of new nanocrystalline cemented carbides. *Powder Metall. Technol.* **40**, 362–375 (2022).
3. Jiang, W. et al. Outstanding high-temperature oxidation- and wear-resistance of WC based cermets. *J. Mater. Sci. Technol.* **155**, 33–46 (2023).
4. Konyashin, I. & Klyachko, L. History of cemented carbides in the Soviet union. *Int. J. Refract. Met. Hard Mater.* **49**, 9–26 (2015).
5. Laptiev, A. Some trends in improving WC–Co hardmetals. I. Hybrid and coarse-grained hardmetals. *Powder Metall. Met. Ceram.* **58**, 42–57 (2019).
6. Dewangan, S., Chattopadhyaya, S. & Hloch, S. Critical damage analysis of WC-Co tip of conical pick due to coal excavation in mines. *Adv. Mater. Sci. Eng.* 292046 (2015).
7. Dewangan, S., Anjan, K., Sagar, N. & Reddy, A. Analysis of critical wear phenomena and stress induced in WC–Co-Based twist Drill Bits used for drilling hard rock. *J. Inst. Eng. (India) Ser. D.* **105**, 689–700 (2024).
8. Li, X., Wang, L., Liu, Y. & Ye, J. Enhanced high temperature mechanical properties of WC-Co cemented carbides by VC addition. *Int. J. Refract. Met. Hard Mater.* **116**, 106355 (2023).
9. Chen, J., Liu, W., Deng, X. & Wu, S. Effects of mo and VC on the microstructure and properties of nano-cemented carbides. *Sci. Sinter.* **48**, 41–50 (2016).
10. Yin, C. et al. Influence of Cr_3C_2 and VC content on WC grain size, WC shape and mechanical properties of WC–6.0 Wt.% Co cemented carbides. *Mater* **14**, 1551 (2021).
11. Yin, C. et al. Effects of Cr_3C_2, VC, and tac on microstructure, WC morphology and mechanical properties of ultrafine WC–10 Wt.% Co cemented carbides. *Met* **10**, 1211 (2020).
12. Zhou, X., Zhang, Z., Li, X., Zhang, X. & Chen, M. Microstructural evolution and mechanical properties of TiC-containing WC-based cemented carbides prepared by pressureless melt infiltration. *Ceram. Int.* **48**, 35115–35126 (2022).
13. Zhai, X. et al. Effects of Nb/TiC/TaC/VC and Co addition on the microstructure and properties of WC-based cemented carbides. *Int. J. Appl. Ceram. Technol.* **20**, 2785–2795 (2023).
14. Ren, X. et al. Effect of ZrC nano-powder addition on the microstructure and mechanical properties of binderless tungsten carbide fabricated by spark plasma sintering. *Int. J. Refract. Met. Hard Mater.* **48**, 398–407 (2015).
15. Jiang, W. et al. Toughening cemented carbides by phase transformation of zirconia. *Mater. Des.* **202**, 109559 (2021).
16. Yang, Y. et al. Study on preparation and properties of WC-8Co cemented carbide doped with rare Earth oxide. *Int. J. Refract. Met. Hard Mater.* **98**, 105536 (2021).
17. Yamanaka, Y. et al. High-resolution transmission electron microscopy study of WC-Co alloy doped with other metal carbides; VC, Cr_3C_2, and ZrC. *Mater. Sci. Forum*. **558–559**, 993–996 (2007).
18. Murugan, N. & Sathiskumar, R. Surface modification and characterization of zirconium carbide particulate reinforced C70600 CuNi composite fabricated via friction stir processing. *J. Mech. Sci. Technol.* **31**, 3755–3760 (2017).
19. Aghaali, V., Ebadzadeh, T., Zahraee, S. & Mirkazemi, S. Microstructure and mechanical properties of WC–TiC–Co cemented carbides produced by spark plasma sintering (SPS) method. *SN Appl. Sci.* **5**, 285 (2023).
20. Gao, Y. et al. Effects of NbC additions on the microstructure and properties of non-uniform structure WC-Co cemented carbides. *Mater. Sci. Eng A*. **687**, 259–268 (2017).

21. Zhou, W. et al. The effect of NbC on mechanical properties and fracture behavior of WC–10Co cemented carbides. *Int. J. Refract. Met. Hard Mater.* **50**, 72–78 (2015).
22. Zulkoski, C., Wijewickreme, D., Honegger, D. & Pipe -CLSM interface bond strength from axial pullout testing. International Pipeline Conference. *Am. Soc. Mech. Eng.* **1**, 86564 (2022).
23. Lubas, M. Au interface effect on Ti-dental porcelain bond strength investigated by spectroscopic methods and mechanical tests. *J. Mol. Struct.* **1208**, 127870 (2020).
24. Hernández-Escobar, D., Slagter, A., Amarillo, S. & Mortensen, A. Room-temperature strength of the interfacial bond between silica inclusions and iron. *Acta Mater.* **263**, 119502 (2024).
25. Yin, Y., Zhai, Z. & Ding, Y. Application of machine learning methods in the analysis of interface bonding strength for over molded hybrid thermoset-thermoplastic composites. *Polym. Compos.* **45**, 8360–8373 (2024).
26. Li, H., Zhang, H. & Jiang, Z. Investigation of the effect of partial Co substitution by Ni and Fe on the interface bond strength of WC cemented carbide based on first-principles calculations. *Mater. Today Commun.* **40**, 109470 (2024).
27. Gren, M., Fransson, E. & Wahnström, G. Computational study of the temperature dependence of interface and surface energies in WC–Co cemented carbides. *Int. J. Refract. Met. Hard Mater.* **87**, 105114 (2020).
28. Cao, R. et al. Interfacial bonding and electronic structure of GaN/GaAs interface: A first-principles study. *J. Appl. Phys.* **117**, 135302 (2015).
29. Mosleh-Shirazi, S., Hua, G., Akhlaghi, F., Yan, X. G. & Li, D. Y. Interfacial Valence electron localization and the corrosion resistance of Al-SiC nanocomposite. *Sci. Rep.* 18154 (2015).
30. Li, D., Guo, L., Li, L. & Lu, H. Electron work function—a probe for interfacial diagnosis. *Sci. Rep.* **7**, 5–6 (2017).
31. Lu, H. et al. Evaluation of interfacial stability and strength of cermets based on work function. *Phys. Chem. Chem. Phys.* **21**, 20706–20719 (2019).
32. Schwanekamp, T. & Reuber, M. Additive manufacturing of application optimized tungsten carbide precision tools. In *6th Int. Conf. Addit. Technol.* 100–114 (2016).
33. Chung, S. R., Wang, K. W., Sheen, S. R., Yeh, C. T. & Perng, T. P. Electrochemical reduction and hydrogenation of Co oxides. *Electrochem. Solid-State Let*. **10**, 155–158 (2007).
34. Ding, S., Zhao, J. & Yu, Q. Effect of zirconia polymorph on vapor-phase ketonization of propionic acid. *Catal* **9**, 768 (2019).
35. Gao, X. et al. Intercalation and controlled release properties of vitamin C intercalated layered double hydroxide. *J. Solid State Chem.* **203**, 174–180 (2013).
36. Baviera, P., Harel, S., Garem, H. & Grosbras, M. Elaboration and structure of nanostructured tic: A XRD and HRTEM study. *Scr. Mater.* **44**, 2721–2727 (2001).
37. Johansson, S. & Wahnström, G. Computational study of thin cubic carbide films in WC/Co interfaces. *Acta Mater.* **59**, 171–181 (2011).
38. Lay, S., Loubradou, M., Johansson, S. & Wahnström, G. Interface structure in a WC–Co alloy co-doped with VC and Cr3C2. *J. Mater. Sci.* **47**, 1588–1593 (2012).
39. Lay, S., Hamar-Thibault, S. & Lackner, A. Location of VC in VC, Cr3C2 codoped WC–Co cermets by HREM and EELS. *Int. J. Refract. Met. Hard Mater.* **20**, 61–69 (2002).
40. Yang, X., Wang, K., Zhang, G. & Chou, K. Fabrication and performances of WC-Co cemented carbide with a low Cobalt content. *Int. J. Appl. Ceram. Technol.* **19**, 1341–1353 (2022).
41. Dutkiewicz, J., Bobrowski, P., Sztukowska, M., Leniewski, W. & Duzews, P. The effect of substitution of WC by tic in WC-Co composite tool materials on microstructure and mechanical properties. *Chiang Mai J. Sci.* **44**, 1714–1721 (2017).

Acknowledgements
This work was supported by the National Natural Science Foundation of China (52301001).

Author contributions
C. W. : Writing – original draft, Methodology, Investigation, Data curation. Z. P. : Formal analysis, Conceptualization, Funding acquisition. Z. Z. : Formal analysis, Validation. X. C. : Formal analysis. K. D. : Writing – review & editing, Project administration, Conceptualization. All authors reviewed the manuscript.

Declarations

Competing interests
The authors declare no competing interests.

Additional information
Correspondence and requests for materials should be addressed to K.D.

Reprints and permissions information is available at www.nature.com/reprints.

Publisher's note Springer Nature remains neutral with regard to jurisdictional claims in published maps and institutional affiliations.